Tuning magnetic and electrical properties in Co doped ZnO films by defect engineering

WANG LIGUO*, ZHANG PEILING
School of Electrical Engineering and Automation, Henan Polytechnic University, Jiaozuo, 454000, People's Republic of China

High quality $Zn_{0.95}Co_{0.05}O$ films with good reproducibility have been prepared by radio-frequency (RF) magnetron sputtering at various preparation conditions. These films were characterized by using x-ray diffraction, electrical transport, and magnetization measurements. The effect of the defects on the structural, magnetic, and electrical properties has been systematically investigated. It was found that the magnetization of $Zn_{0.95}Co_{0.05}O$ films increases with increasing defects, whereas the resistivity decreases with increasing defects. The observed correlation between the magnetization, carrier concentration, and defects demonstrated the effect of the defects in controlling the magnetic and electrical properties in $Zn_{0.95}Co_{0.05}O$ films. This also indicated that the magnetic and electrical properties of $Zn_{0.95}Co_{0.05}O$ films can be tuned by defect engineering.

(Received July 9, 2012; accepted March 13, 2014)

Keywords: Magnetic property, Electrical property, Defect engineering

1. Introduction

Diluted magnetic semiconductors (DMSs) have attracted much attention for their potential applications in spintronics [1–3]. Investigations on the DMSs were originally inspired by the discovery of spontaneous low temperature ferromagnetism in Mn-doped GaAs exhibiting a Curie temperature (T_C) of about 110 K [1]. In contrast to III-V-based DMSs with a low T_C, room temperature (RT) ferromagnetism was theoretically predicted to be realizable in p-type Mn doped ZnO or in n-type Co doped ZnO [4, 5]. As one of the most promising candidates to obtain RT ferromagnetism, ZnO-based DMSs with transition metal (TM) have been extensively investigated [6–18]. Despite RT ferromagnetism has been observed in ZnO-based DMSs, there are still many controversies remained on the physical origin and /or mechanism of the observed ferromagnetism. In several cases the ferromagnetism observed was attributed to uncontrolled ferromagnetic clusters or secondary phases [9, 10]. However, there are strong evidences that the TM atoms substitute for Zn sites in the ZnO lattice without changing the wurtzite structure, and it is possible that no segregation of secondary phase exists [11, 12]. Further research works have documented that the appearance of ferromagnetism in TM doped ZnO samples can be caused by additional carriers [13, 14], as explained by the carrier-mediated exchange mechanism [15]. Meanwhile, Coey et al. proposed that the ferromagnetic coupling in oxide-based DMSs is mediated by shallow donor defect through forming bound magnetic polarons (BMPs) [16], and indeed there are some reports about relations between ferromagnetism and defects [17, 18]. Furthermore, RT ferromagnetism was observed in oxides or semiconductors doped with nonmagnetic elements as well as undoped oxides such as ZnO, TiO_2, and In_2O_3, etc [19–21], and the magnetic properties of these materials are strongly dependent on sample preparation. These results give an indication that the defects may play an important role in the observed magnetic behaviors of the DMSs. Therefore, how to control and engineer defects becomes a very interesting and important issue. It will be very useful if the defects can be manipulated to improve the properties of these DMS materials.

In this work, we prepared $Zn_{0.95}Co_{0.05}O$ films with good reproducibility by radio-frequency (RF) magnetron sputtering at various preparation conditions, and strong magnetic and electrical properties depending on the preparation conditions was observed, showing that these properties are strongly correlated with the defects. Simultaneously, we found that the magnetic and electrical properties may be tailored in $Zn_{0.95}Co_{0.05}O$ films because a large amount of defects.

2. Experiment

A high dense ceramic $Zn_{0.95}Co_{0.05}O$ target was prepared by solid state reaction method using pure ZnO (99.999%) and CoO (99.999%) powders in stoichiometric ratios. $Zn_{0.95}Co_{0.05}O$ thin films were grown on Si (100) substrates by using radio-frequency (RF) magnetron sputtering at various preparation conditions. The base pressure of the deposition chamber is below 2×10^{-5} Pa. The deposition was performed in a total working pressure of 0.65 Pa, which is a mixture of argon (Ar) partial pressures and oxygen (O_2) partial pressures. Using a capacitance gauge, the total Ar and O_2 pressure was monitored precisely. For each run, the total pressure during presputtering in Ar only (p_1) and during deposition in Ar and O_2 (p_2) were determined. The oxygen partial pressure during film deposition was calculated as $p_{O_2} = p_2 - p_1$.

The sample thickness was measured using a Dektak profilometer, and the thickness of all the samples was controlled by the deposition time. The structure and crystalline quality of the samples were determined by x-ray diffraction (XRD) using Cu Kα radiation. The magnetic properties were measured using a vibrating sample magnetometer with the magnetic field applied parallel to the film plane. Electrical transport including Hall measurements was carried out using a four terminal van der Pauw configuration.

3. Results and discussions

The XRD pattern of a 120nm-thick $Zn_{0.95}Co_{0.05}O$ film deposited on Si (100) substrate under oxygen partial pressure $p_{O_2} = 0.15$ Pa and substrate temperature $T_S = 450$ ℃ are shown in Fig. 1. It can be seen that the $Zn_{0.95}Co_{0.05}O$ sample has a single ZnO wurtzite structure with c-axis preferred orientation. The intense and sharp peaks observed indicated that the $Zn_{0.95}Co_{0.05}O$ film is highly crystallized. Moreover, no diffraction peaks corresponding to the Co-related secondary phases were detected, which implies that the Co atoms in our sample substitute for Zn atoms in the ZnO lattice without changing the wurtzite structure.

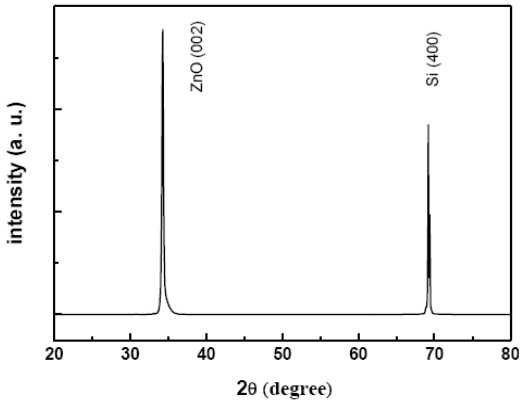

Fig. 1. XRD pattern of a 120nm-thick $Zn_{0.95}Co_{0.05}O$ film deposited on Si (100) substrate under oxygen partial pressure $p_{O_2} = 0.15$ Pa and substrate temperature $T_S = 450$ ℃.

The magnetic measurements of 120 nm-thick $Zn_{0.95}Co_{0.05}O$ films deposited under different p_{O_2} and $T_S = 450$ ℃ have been performed at room temperature, as shown in Fig. 2. It is clear from the figure that the magnetic property of all the films is quite different when they were deposited under different p_{O_2}. The magnetic moments are 0.61, 0.35, 0.27, and 0.12 μ_B / Co for the samples deposited under the $p_{O_2} = 0$ Pa, 0.075 Pa, 0.15 Pa, and 0.225 Pa, respectively. The result suggests that the magnetic property of $Zn_{0.95}Co_{0.05}O$ films is dependent on the p_{O_2}, and sharply decrease with increasing p_{O_2}. Similar results have been found in other oxide DMSs such as Mn-doped ZnO, Co-doped TiO_2, and In_2O_3, etc [22–24]. The dependence of magnetization of $Zn_{0.95}Co_{0.05}O$ films on the p_{O_2} can be understood as follows. When $Zn_{0.95}Co_{0.05}O$ films are deposited under low p_{O_2}, oxygen atoms are readily lost to the external environment, thereby, creating oxygen vacancies. While at high p_{O_2}, a large amount of oxygen is introduced during the deposition process, it acts to prevent the formation of oxygen vacancies. On the other hand, the film growth rate increases with decreasing p_{O_2}, accompanied by the

increase of structural defects such as edge dislocation and stacking faults. Therefore, it can be deduced that the magnetic behaviors in $Zn_{0.95}Co_{0.05}O$ films are strongly related with the defects.

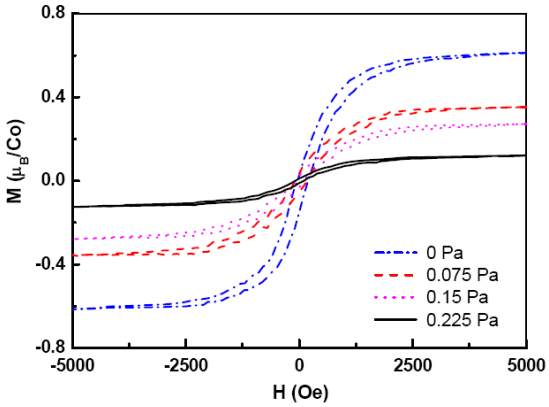

Fig. 2. Magnetization hysteresis curves of 120nm-thick $Zn_{0.95}Co_{0.05}O$ films deposited under different p_{O_2} and $T_S = 450$ ℃ measured at room temperature.

It is known that ZnO is very easily and naturally an n-type semiconductor due to the existence of native defects. To investigate the electrical properties of $Zn_{0.95}Co_{0.05}O$ films deposited under various p_{O_2}, we preformed the RT measurements of the resistivity and Hall effect, as summarized in Table 1. The RT resistivities are 0.016, 0.082, 0.271, and 33.7 Ωcm for the samples deposited under the $p_{O_2} = 0$ Pa, 0.075 Pa, 0.15 Pa, and 0.225 Pa, respectively, and the corresponding carrier densities are 6.35×10^{19}, 1.01×10^{19}, 8.68×10^{18}, and 9.12×10^{16} cm^{-3}. It can be found that the p_{O_2} has also a profound influence on the electrical properties of $Zn_{0.95}Co_{0.05}O$ films. With the increase of the p_{O_2}, the resistivity sharply increases, and the carrier concentration correspondingly decreases. This can be attributed to a decreasing density of oxygen vacancies acting as electron donors caused by an excess of oxygen during film deposition, which will lead to a decrease of the electron concentration. The variation of the resistivity and carrier concentration with the p_{O_2} indicated that the electrical properties in $Zn_{0.95}Co_{0.05}O$ films are also closely related to the defects. Furthermore, the c-axis lattice constant of $Zn_{0.95}Co_{0.05}O$ films deposited under various p_{O_2} calculated from XRD data is also summarized in Table 1. It should be emphasized that these values of c-axis lattice constant for $Zn_{0.95}Co_{0.05}O$ films deposited under various p_{O_2} are larger than that of undoped wurtzite ZnO (5.207 Å). On the other hand, it is clear that the p_{O_2} has also a slight influence on the c-axis lattice constant of $Zn_{0.95}Co_{0.05}O$ films. With the decrease of the p_{O_2}, the c-axis lattice constant gradually increases from 5.253 Å to 5.364 Å, indicating that the unit cell of $Zn_{0.95}Co_{0.05}O$ film is elongated along the c-axis. This also further shown that the electrical and magnetic behaviors of $Zn_{0.95}Co_{0.05}O$ films are related with the defects.

Table 1. The c-axis lattice constant, resistivity, carrier concentration, and saturated magnetization (M_s) of 120nm-thick $Zn_{0.95}Co_{0.05}O$ films deposited under different p_{O_2} and $T_S = 450$ ℃ measured at room temperature.

Sample	c-axis lattice constant (Å)	Resistivity (Ω cm)	Carrier concentration (cm^{-3})	M_s (μ_B/Co)
$p_{O_2} = 0$ Pa	5.364	0.016	6.35×10^{19}	0.61
$p_{O_2} = 0.075$ Pa	5.316	0.082	1.01×10^{19}	0.35
$p_{O_2} = 0.15$ Pa	5.278	0.271	8.68×10^{18}	0.27
$p_{O_2} = 0.225$ Pa	5.253	33.7	9.12×10^{16}	0.12

In order to further investigate the effect of the defects on the magnetic behavior of $Zn_{0.95}Co_{0.05}O$ films, we performed the RT magnetic measurements on the films with different thicknesses deposited under $p_{O_2} = 0.075$ Pa and $T_S = 450$ ℃, as shown in Fig. 3. It is clear that the saturated magnetization rapidly decreases with the increase in film thickness. It was noted that the 10 nm-thick film shows giant magnetic moment, i.e. 1.24 μ_B / Co, which is close to that of Co metal (1.7 μ_B / Co). However, the 500 nm-thick sample shows a weak magnetization of 0.06 μ_B / Co, which is much smaller than that of the 10 nm-thick sample. For the thickness-dependent magnetization of our $Zn_{0.95}Co_{0.05}O$ films, it can be understood as follows. Large strain exists in the thin $Zn_{0.95}Co_{0.05}O$ films due to the lattice mismatches between the film and the substrate, which will lead to a large number of defects in the film. As the film thickness increases, the strain in the film rapidly decreases and fewer defects are generated.

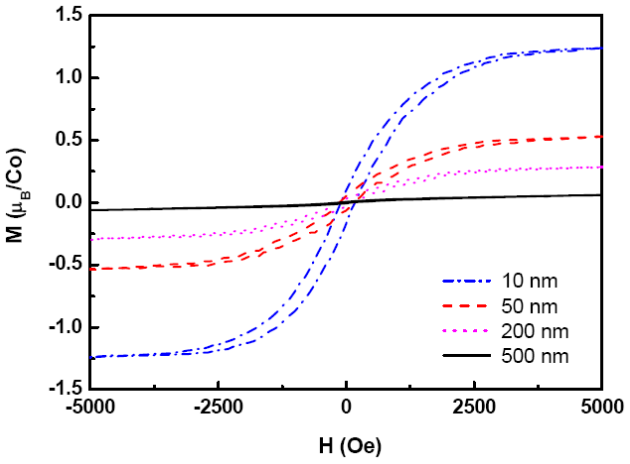

Fig. 3. Magnetization hysteresis curves of $Zn_{0.95}Co_{0.05}O$ films with different thicknesses deposited under $p_{O_2} = 0.075$ Pa and $T_S = 450$ ℃ measured at room temperature.

It should be noted that the magnetic behaviors and electrical properties also vary with substrate temperature. Fig. 4 shows the RT magnetization hysteresis loops of 120nm-thick $Zn_{0.95}Co_{0.05}O$ films deposited under $p_{O_2} = 0.075$ Pa and different substrate temperature. The magnetic moment gradually decreases with increasing substrate temperature. We know that the crystallinity of films can be improved by increasing substrate temperature, which can depress the structural defects such as edge dislocation and stacking faults. Meanwhile, the point defects, i.e., oxygen vacancies and Zn interstitials, derived from the structural defects are reduced as a consequence. This is consistent with the enhancement of the crystalline quality of Co:ZnO films by annealing [25]. These results showed that the magnetic moment decreases with an improvement in crystallinity, indicating that the magnetization of $Zn_{0.95}Co_{0.05}O$ films is strongly correlated with the defects, which supports the concept of Hong et al. that the RT ferromagnetism of TM-doped ZnO likely arises from structural defects [26]. To better understand the properties of $Zn_{0.95}Co_{0.05}O$ films deposited at different substrate temperature, we also performed the c-axis lattice constant calculations and RT resistivity and Hall effect measurements, as shown in Table 2. It was found that the substrate temperature has a slight influence on the structural and electrical properties of $Zn_{0.95}Co_{0.05}O$ films. With the increase of the substrate temperature, the c-axis lattice constant slightly decreases, while the resistivity gradually increases (the corresponding carrier concentration continuously decreases). Based on these results, it was further confirmed that the magnetic and electrical behaviors in $Zn_{0.95}Co_{0.05}O$ films are dependent on the defects.

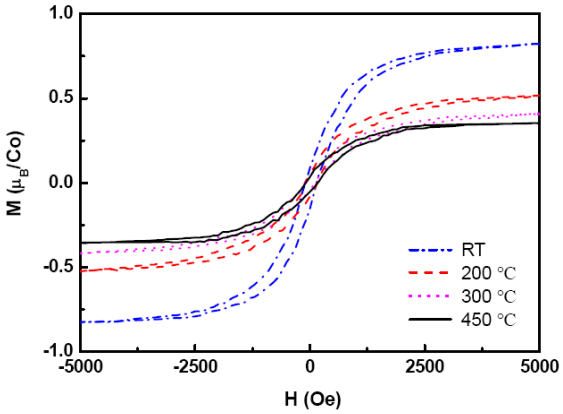

Fig. 4. Magnetization hysteresis curves of 120nm-thick $Zn_{0.95}Co_{0.05}O$ films deposited under $p_{O_2} = 0.075$ Pa and different T_S measured at room temperature.

Table 2. The c-axis lattice constant, resistivity, carrier concentration, and saturated magnetization (M_s) of 120nm-thick $Zn_{0.95}Co_{0.05}O$ films deposited under $p_{O_2} = 0.075$ Pa and different T_S measured at roomtemperature.

Sample	c-axis lattice constant (Å)	Resistivity (Ω cm)	Carrier concentration (cm^{-3})	M_s (μ_B/Co)
RT	5.385	0.012	8.19×10^{19}	0.82
$T_S = 200$ ℃	5.347	0.038	3.23×10^{19}	0.52
$T_S = 300$ ℃	5.332	0.051	2.55×10^{19}	0.41
$T_S = 450$ ℃	5.316	0.082	1.01×10^{19}	0.35

Combining the above structural, magnetic, and electrical measurement results, it can be concluded that the magnetic and electrical properties in $Zn_{0.95}Co_{0.05}O$ films are strongly related with the defects, indicating the magnetic and electrical behaviors can be tuned by changing the defect amount. These results can be well comprehended in the framework of the bound magnetic polaron (BMP) model based on the presence of defects [16]. According to the BMP model, the ferromagnetic exchange is mediated by donor electrons through forming BMPs, while the defects would be responsible for generating carriers. In our $Zn_{0.95}Co_{0.05}O$ films, it is possible that the defects are located at arbitrary distances with respect to the Co sites. The donor spin of a defect correlating with Co^{2+} within its orbit mediates effective interactions between them, and the shaped BMPs try to spread out to overlap and interact with adjacent BMPs to realize magnetic ordering.

4. Conclusion

In summary, high quality $Zn_{0.95}Co_{0.05}O$ thin films with c-axis orientation were prepared by RF magnetron sputtering at various preparation conditions. The effect of the defects on the structural, magnetic, and electrical properties of $Zn_{0.95}Co_{0.05}O$ films was investigated. The experimental results showed a clear correlation between the magnetic properties, the electrical properties, and the preparation conditions. It was found that the magnetization of $Zn_{0.95}Co_{0.05}O$ films increases with increasing defects, whereas the resistivity decreases with increasing defects. This indicated that the magnetic and electrical properties of $Zn_{0.95}Co_{0.05}O$ films can be tuned by controlling the defects. Meanwhile, these results presented here implied that the defect amount in $Zn_{0.95}Co_{0.05}O$ films is strongly correlated with the observed magnetization confirming the mechanism of bound magnetic polaron. Finally, our findings are helpful for designing useful functional materials for spintronic devices and for understanding the ferromagnetic mechanism in oxide-based diluted magnetic semiconductors.

References

[1] H. Ohno, Science **281**, 951 (1998).
[2] S. A. Wolf, D. D. Awschalom, R. A. Buhrman, J. M. Daughton, S. V. Molnar, M. L. Roukes, A. Y. Chtchelkanova, D. M. Treger, Science **294**, 1488 (2001).
[3] S. J. Pearton, C. R. Abernathy, M. E. Overberg, G. T. Thaler, D. P. Norton, N. Theodoropoulou, A. F. Hebard, Y. D. Park, F. Ren, J. Kim, L. A. Boatner, J. Appl. Phys. **93**, 1 (2003).
[4] T. Dietl, H. Ohno, F. Matsukura, J. Cubert, D. Ferrand, Science **287**, 1019 (2000).
[5] K. Sato, H. Katyama-Yoshida, Semicond. Sci. Technol. **17**, 367 (2002).
[6] A. J. Behan, A. Mokhtari, H. J. Blythe, D. Score, X. H. Xu, J. R. Neal, A. M. Fox, G. A. Gehring, Phys. Rev. Lett. **100**, 047206 (2008).
[7] J. B. Yi, C. C. Lim, G. Z. Xing, H. M. Fan, L. H. Van, S. L. Huang, K. S. Yang, X. L. Huang, X. B. Qin, B. Y. Wang, T. Wu, L. Wang, H. T. Zhang, X. Y. Gao, T. Liu, A. T. S. Wee, Y. P. Feng, J. Ding, Phys. Rev. Lett. **104**, 137201 (2010).
[8] H. Gu, Y. Z. Jiang, Y. B. Xu, M. Yan, Appl. Phys. Lett. **98**, 012502 (2011).
[9] K. Rode, R. Mattana, A. Anane, V. Cros, E. Jacquet, J. P. Contour, F. Petroff, A. Fert, Appl. Phys. Lett. **92**, 012509 (2008).
[10] M. Snure, D. Kumar, A. Tiwari, Appl. Phys. Lett. **94**, 012510 (2009).
[11] K. Ueda, H. Tabat, T. Kawai, Appl. Phys. Lett. **79**, 988 (2001).
[12] S. Ramachandran, A. Tiwari, J. Narayan, Appl. Phys.

Lett. **84**, 5255 (2004).
[13] Q. Wana, Appl. Phys. Lett. **89**, 082515 (2006).
[14] D. L. Zhou, X. J. Ye, H. J. Meng, H. J. Zhou, X. L. Li, C. M. Zhen, G. D. Tang, Appl. Phys. Lett. **90**, 142502 (2007).
[15] A. Walsh, J. L. F. Da Silva, S. H. Wei, Phys. Rev. Lett. **100**, 256401 (2008).
[16] J. M. D. Coey, M. Venkatesan, C. B. Fitzgerald, Nature Mater. **4**, 173 (2005).
[17] H. S. Hsu, J. C. A. Huang, Appl. Phys. Lett. **88**, 242507 (2006).
[18] Q. Xu, H. Schmidt, S. Zhou, K. Potzger, M. Helm, H. Hochmuth, M. Lorenz, A. Setzer, P. Esquinazi, C. Meinecke, M. Grundmann, Appl. Phys. Lett. **92**, 082508 (2008).
[19] H. Pan, J. B. Yi, L. Shen, R. Q. Wu, J. H. Yang, J. Y. Lin, Y. P. Feng, J. Ding, L. H. Van, J. H. Yin, Phys. Rev. Lett. **99**, 127201 (2007).
[20] N. H. Hong, J. Sakai, N. Poirot, V. Brizé, Phys. Rev. B **73**, 132404 (2006).
[21] M. Venkatesan, C. B. Fitzgerald, J. M. D. Coey, Nature (London) **430**, 630 (2004).
[22] S. Ramachandran, J. Naryan, J. T. Prater, Appl. Phys.Lett. **88**, 242503 (2006).
[23] A. Manivannan, G. Glaspell, P. Dutta, M. S. Seehra, J. Appl. Phys. **97**, 10D325 (2005).
[24] J. Philip, A. Punnoose, B. I. Kim, K. M. Reddy, S. Layne, J. O. Holmes, B. Satpati, P. R. Leclair, T. S. Santos, J. S. Moodera, Nat. Mater. **5**, 298 (2006).
[25] C. Song，S. N. Pan, X. J. Liu, X. W. Li, F. Zeng, W. S. Yan, B. He, F. Pan, J. Phys.: Condens. Matter **19**, 176229 (2007).
[26] N. H. Hong, J. Sakai, N. T. Huong, N. Poirot, A. Ruyter, Phys. Rev. B **72**, 045336 (2005).

*Corresponding author: wanglg23@163.com